

Bridging the gap between seismic and sub seismic Mirror Slip Surfaces in Carbonate Fault Gouge

Milo Trainor Moss¹, Berend A. Verberne², Miki Takahashi² and Andre R. Niemeijer¹

¹Utrecht University, Department of Earth Science, Netherlands

²Geological Survey of Japan, National Institute of Industrial Science and Technology, Tsukuba, Ibaraki, Japan

Contact: m.trainormoss@students.uu.nl

European Geoscience Union 2020 : Sharing Geoscience Online - May 5, 2020
Session TS5.3 - The Mechanics of Earthquake Faulting: a multiscale approach



- Highly reflective fault mirrors are widely observed in tectonically active carbonate terrains
- 'Shinny' or 'Mirror like' Slip Surfaces (MSS) have been experimentally produced at both seismic ($v \geq 10^{-4} \text{ ms}^{-1}$) and sub seismic slip velocities ($v < 10^{-4} \text{ ms}^{-1}$)
- MSS produced at seismic slip velocities at a range of normal stress ($\sigma_n^{\text{eff}} = 0.9 - 28.4 \text{ MPa}$) (Siman-Tov et al., 2015; Green II et al., 2015)
- Role of normal stress at sub seismic velocities yet to be investigated
- MSS produced at seismic and sub seismic velocities are internally composed of nanogranular material (Siman-Tov et al., 2013; Verberne et al., 2014)

Aim

- Investigate the effect of normal stress (σ_n^{eff}) & cumulative displacement (Σx) on MSS development at sub seismic slip velocities
- Are there distinguishing characteristics between MSS produced at sub seismic and seismic slip velocities
 - > Can natural MSS be used to identify paeloseismic slip?
- Investigate whether MSS can be reproduced under the same conditions with different deformation apparatuses

Experimental set up

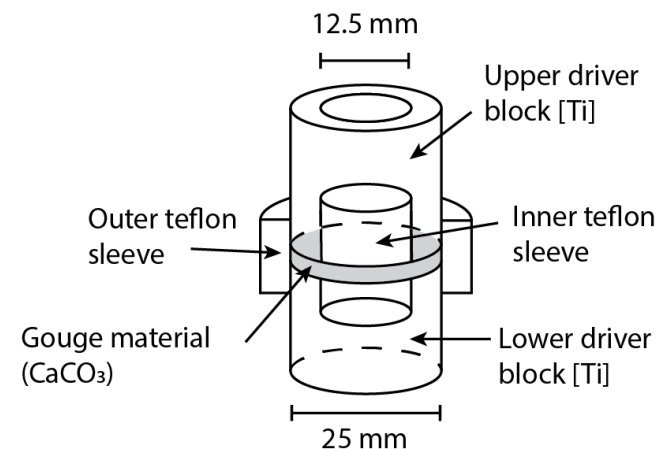
- Calcite fault gouge ($d = 12\text{-}15\ \mu\text{m}$)
- Argo gas Triaxial Deformation Apparatus with a saw cut assembly
- Rotary Shear Apparatus
- All experiments performed at room dry conditions and room temperature
- Microstructural analysis – visual inspection, light microscopy and SEM
- Raman spectroscopy

Triaxial Deformation Apparatus

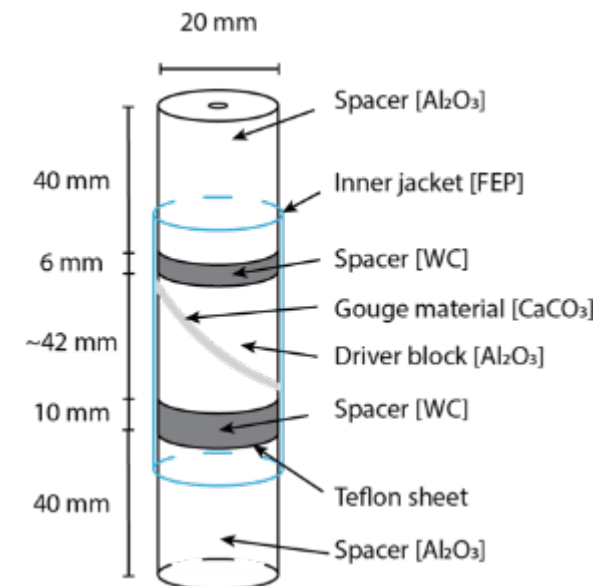
Velocity = $10^{-6}\ \text{ms}^{-1}$

Σx [mm] / P_c [MPa]	1.6	3.6	5.6
6 ($\sigma_n^{\text{eff}} \approx 10$)			
30 ($\sigma_n^{\text{eff}} \approx 50$)			
100 ($\sigma_n^{\text{eff}} \approx 170$)			

Rotary Shear Assembly



Saw cut Assembly



Rotary Shear Apparatus

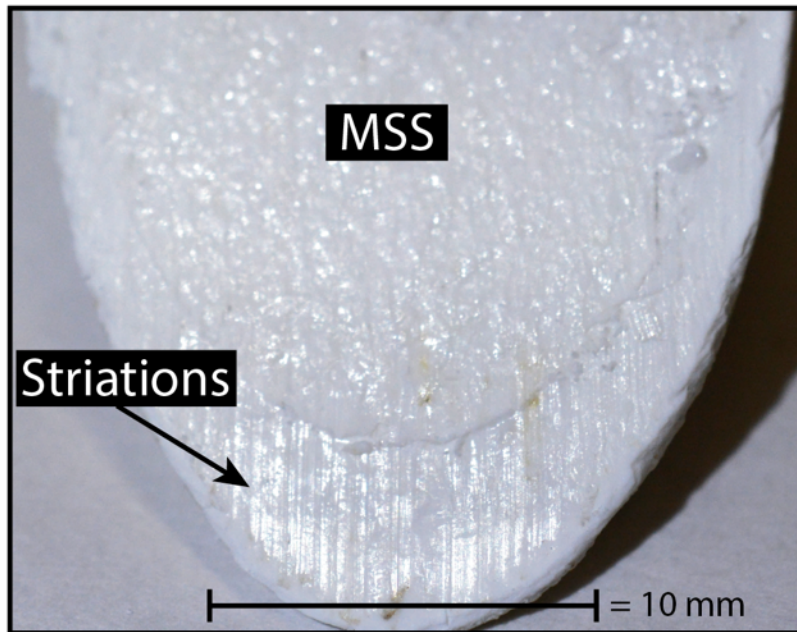
$\sigma_n^{\text{eff}} = 10\ \text{MPa}$

Σx [mm] / Velocity	6	20	50
$10^{-6}\ \text{ms}^{-1}$			
$10^{-5}\ \text{ms}^{-1}$			
$10^{-4}\ \text{ms}^{-1}$			
$10^{-3}\ \text{ms}^{-1}$			

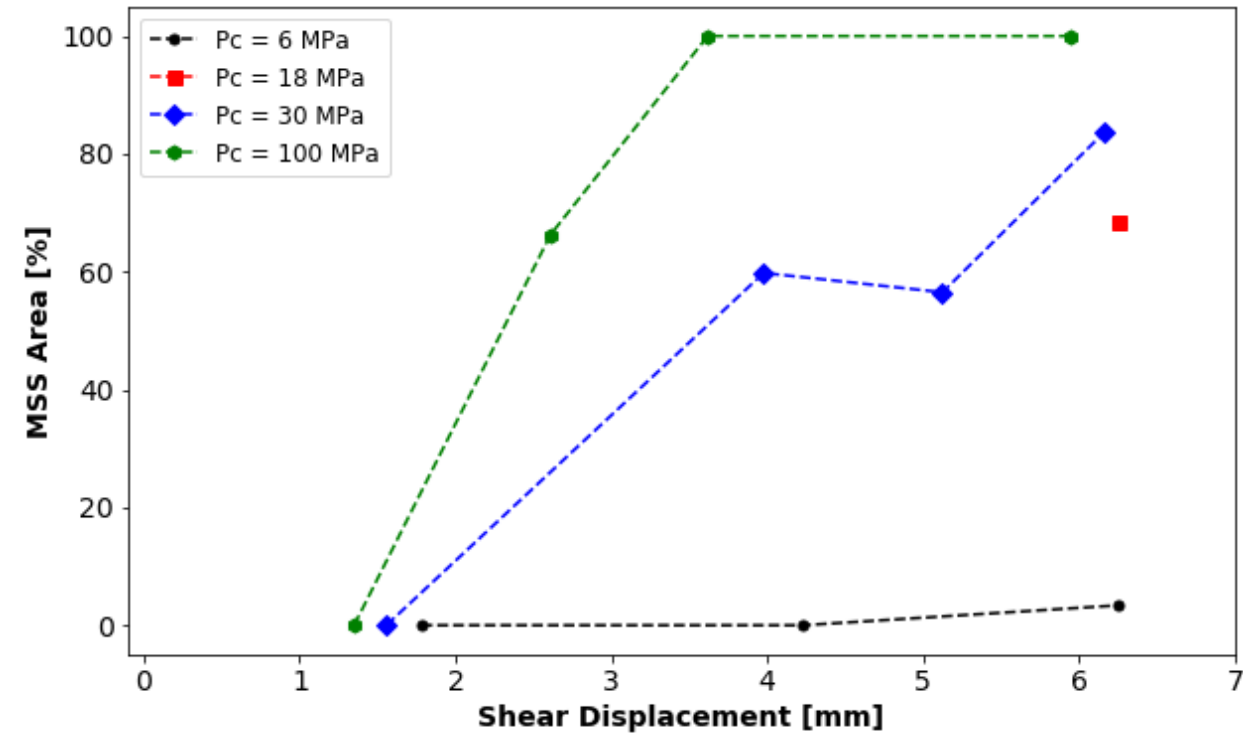
Rotary Shear Apparatus

v [ms^{-1}]	σ_n^{eff} [MPa]	Σx [m]
0.26	1.5	3.7
1.2	10	1

- MSS exposed along boundary shear between driver block and gouge
- Areal extent of the MSS systematically increases with displacement
- The displacement after which MSS develop rapidly decreases as confining pressure (normal stress) is increased



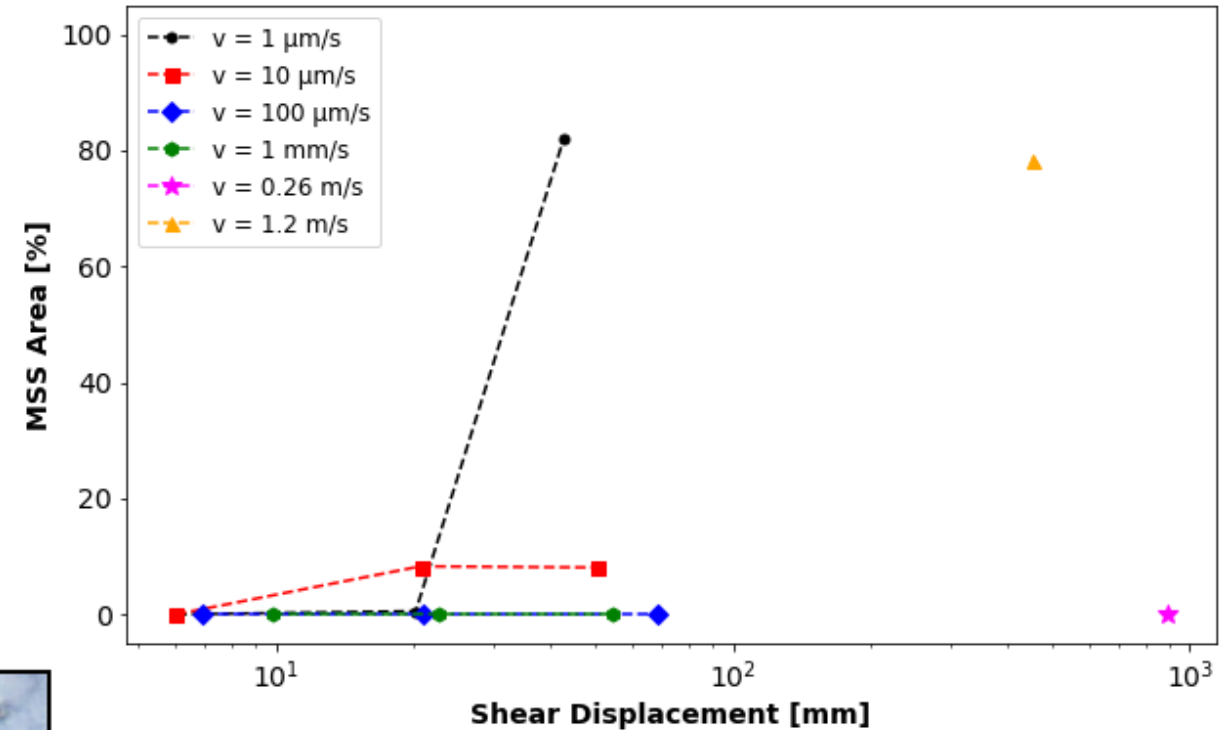
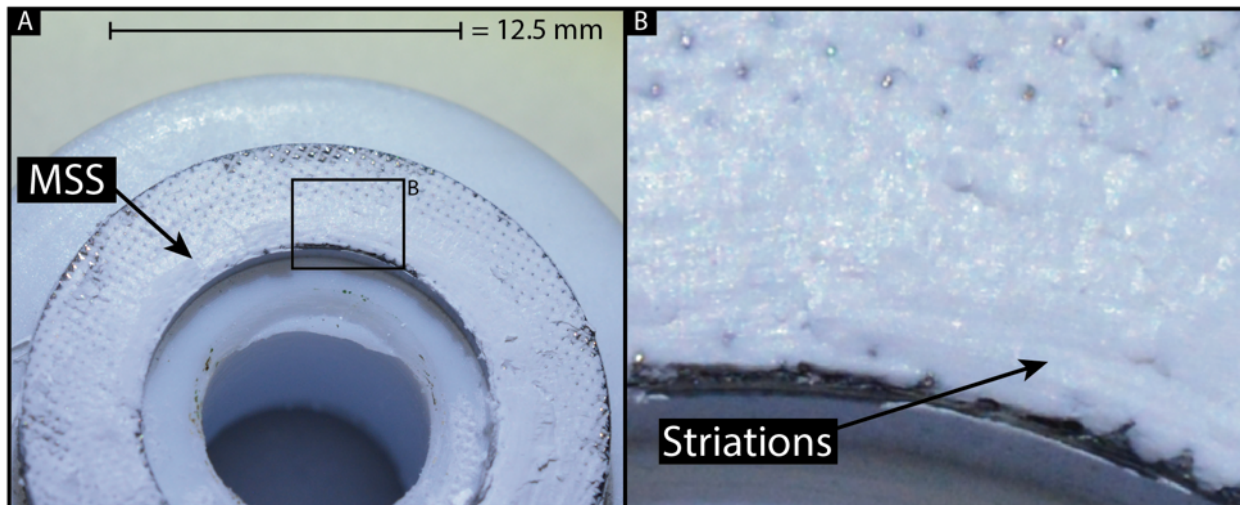
Photograph of MSS:
 $P_c = 30 \text{ MPa}$
 $(\sigma_n^{\text{eff}} = 52 \text{ MPa})$
 $v = 10^{-6} \text{ ms}^{-1}$
 $\Sigma x = 6.16 \text{ mm}$



$$\text{MSS Area [\%]} = \frac{\text{Area of MSS}}{\text{Area of Sample recovered}} * 100$$

- Patchy = MSS Area < 80%
- Continuous = MSS Area > 80%

- MSS exposed along the boundary shear between the sample and lower driver block
- MSS observed at $v = 10^{-6}$ & 10^{-5} ms^{-1} but not at $v = 10^{-4}$ & 10^{-3} ms^{-1}
- MSS reappear at seismic slip velocities ($v = 1.2 \text{ ms}^{-1}$)
- Unlike in the triaxial experiments MSS were not observed after 6 mm of displacement at $v = 10^{-6} \text{ ms}^{-1}$ and $\sigma_n^{\text{eff}} = 10 \text{ MPa}$



Photograph of MSS exposed on lower driver block:
 $\sigma_n^{\text{eff}} = 10 \text{ MPa}$
 $v = 10^{-6} \text{ ms}^{-1}$
 $\Sigma x = 42.67 \text{ mm}$

- Patchy = MSS Area < 80%
- Continuous = MSS Area > 80%

MSS produced at seismic and sub seismic slip velocities are internally composed of rounded nanospherules ($d \approx 100\text{nm}$)

Nanospherules sinter to form low porosity MSS

Holes in the MSS expose the more porous shear band below the MSS which is also composed of nanospherules

MSS produced at sub seismic velocities, low normal stresses and high displacements display poor sintering and a noticeably higher porosity

MSS produced at seismic velocities display a remarkably lower porosity and more enhanced sintering



$P_c = 30 \text{ MPa}$ ($\sigma_n^{\text{eff}} = 54 \text{ MPa}$), $v = 10^{-6} \text{ ms}^{-1}$, $\Sigma x = 3.98 \text{ mm}$	$P_c = 18 \text{ MPa}$ ($\sigma_n^{\text{eff}} = 32 \text{ MPa}$), $v = 10^{-6} \text{ ms}^{-1}$, $\Sigma x = 6.25 \text{ mm}$	$\sigma_n^{\text{eff}} = 10 \text{ MPa}$, $v = 10^{-6} \text{ ms}^{-1}$, $\Sigma x = 42.67 \text{ mm}$	$\sigma_n^{\text{eff}} = 10 \text{ MPa}$, $v = 1.2 \text{ ms}^{-1}$, $\Sigma x = 453.98 \text{ mm}$
---	---	--	---

Triaxial deformation apparatus

Rotary shear apparatus

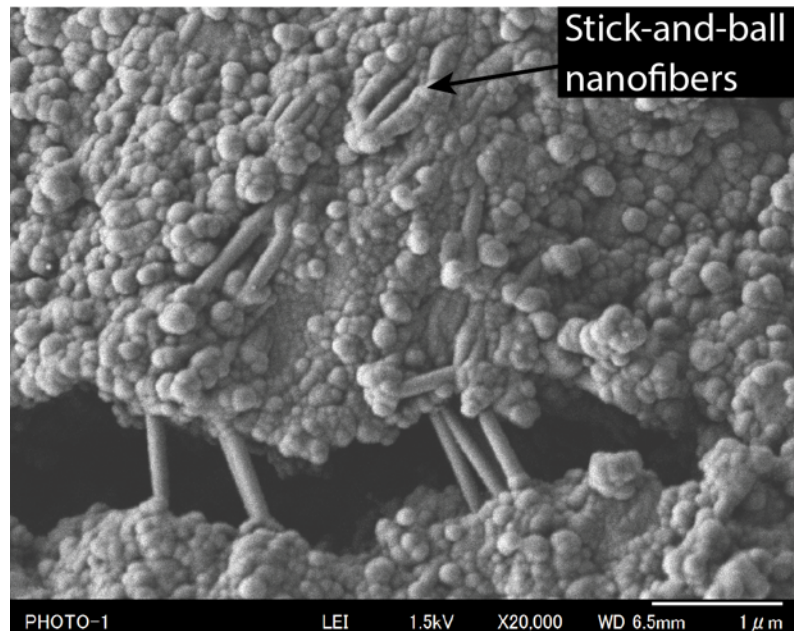
Nanofibrous structures observed in:

Triaxial experiments performed at 10^{-6} ms^{-1} at $\sigma_n^{\text{eff}} \approx 50 \text{ MPa}$ & 170 MPa

Rotary shear experiments performed 10^{-5} ms^{-1} at $\sigma_n^{\text{eff}} = 10 \text{ MPa}$

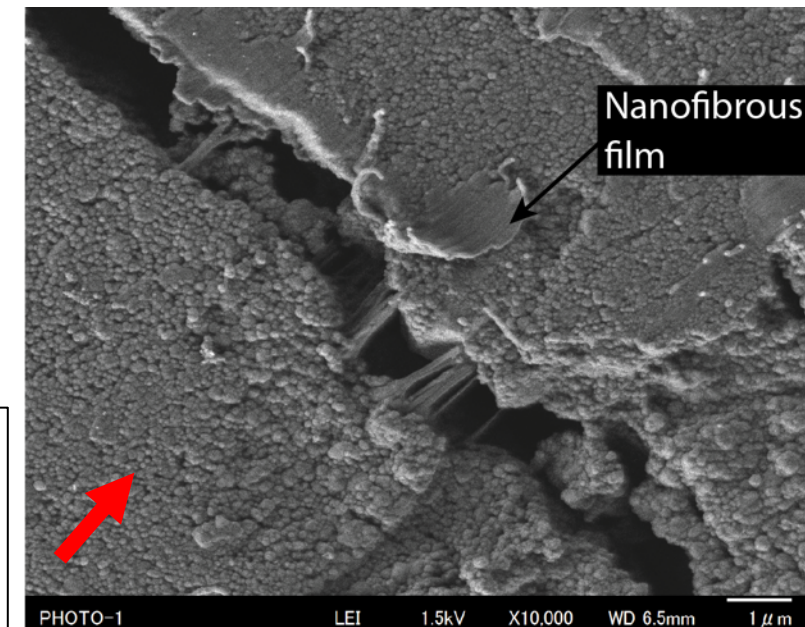
- Nanofibers connect individual nanospherules produced a 'stick-and-ball' structure.
- Individual nanofibers observed in fractures in the MSS and within the MSS
- In the experiments performed at high normal stress ($\sigma_n^{\text{eff}} \approx 170 \text{ MPa}$) nanofibrous films composed aligned nanofibers were also observed which align with the slip direction

Stick-and-ball nanofibers



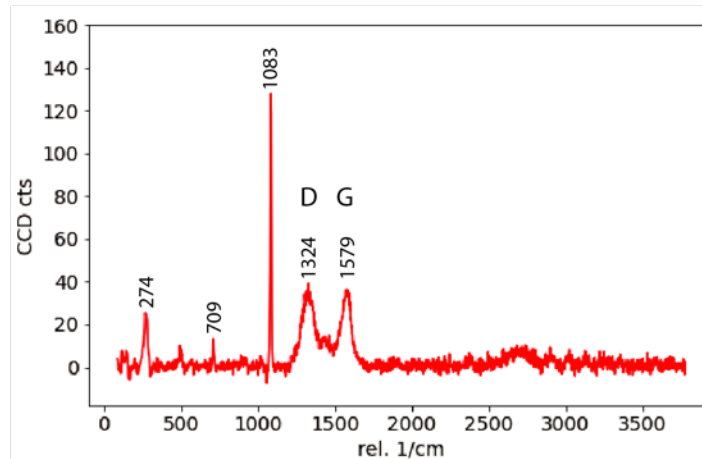
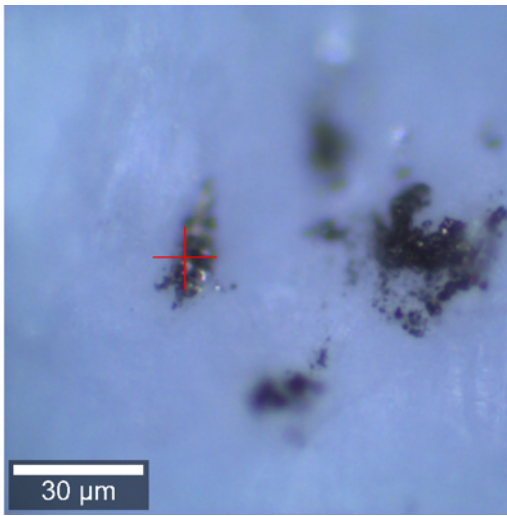
$P_c = 30 \text{ MPa}$
 $(\sigma_n^{\text{eff}} = 54 \text{ MPa})$
 $v = 10^{-6} \text{ ms}^{-1}$
 $\Sigma x = 3.98 \text{ mm}$

Nanofibrous films

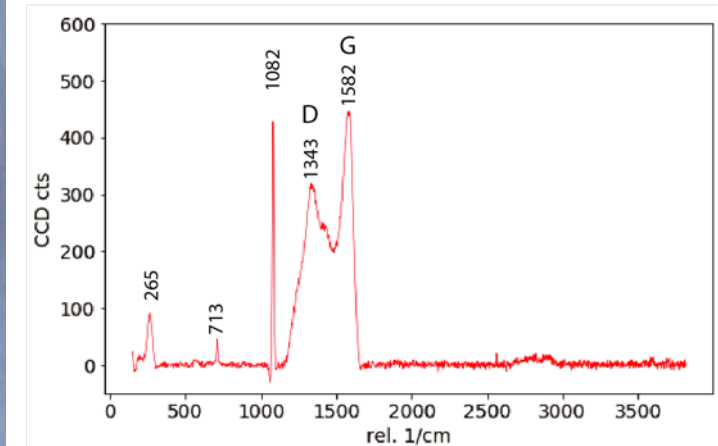
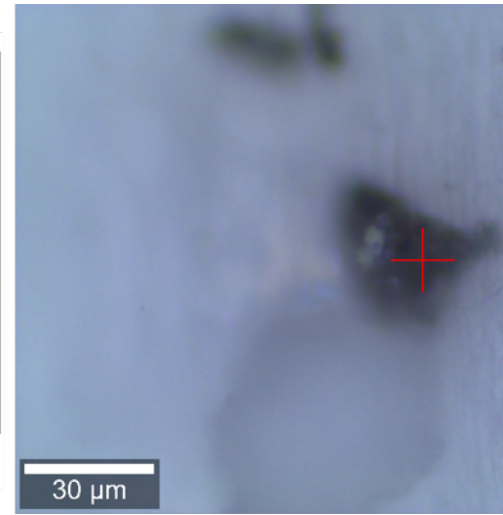


$P_c = 100 \text{ MPa}$
 $(\sigma_n^{\text{eff}} = 160 \text{ MPa})$
 $v = 10^{-6} \text{ ms}^{-1}$
 $\Sigma x = 5.95 \text{ mm}$

- MSS produced at sub seismic and seismic slip velocities composed of crystalline calcite
- Patches of Amorphous Carbon observed on MSS produced in all experiments performed at $v = 10^{-6} \text{ ms}^{-1}$, $P_c = 100 \text{ MPa}$ ($\sigma_n^{\text{eff}} \approx 170 \text{ MPa}$)
- No measured macroscopic temperature rise at $v = 10^{-6} \text{ ms}^{-1}$
- Patch/ fragments of Amorphous Carbon on top of MSS produced at $v = 1.2 \text{ ms}^{-1}$, $\sigma_n^{\text{eff}} = 10 \text{ MPa}$, $\Sigma x = 453.98 \text{ mm}$

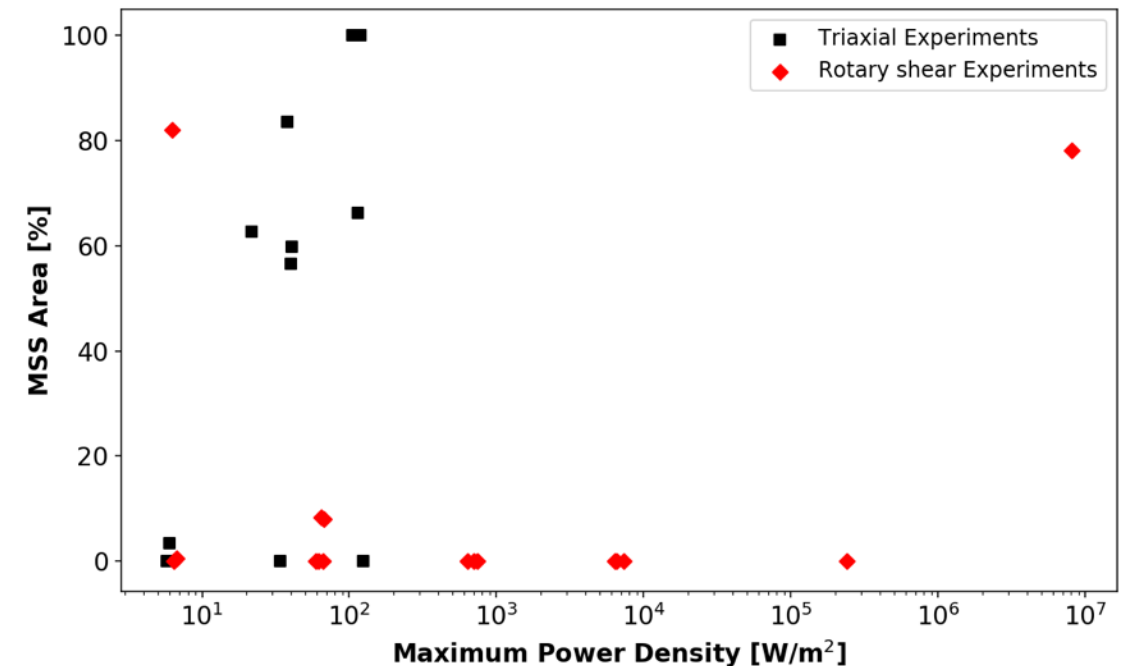


$v = 10^{-6} \text{ ms}^{-1}$, $P_c = 100 \text{ MPa}$ ($\sigma_n^{\text{eff}} = 166 \text{ MPa}$),
 $\Sigma x = 2.61 \text{ mm}$



$v = 1.2 \text{ ms}^{-1}$, $\sigma_n^{\text{eff}} = 10 \text{ MPa}$, $\Sigma x = 453.98 \text{ mm}$

- Continuous MSS were produced (>80% of sample is MSS) at both seismic and sub seismic velocities
- MSS are low porosity layers composed of rounded nanospherules
- MSS Area systematically increases with displacement at sub seismic slip velocities ($v = 10^{-6} \text{ ms}^{-1}$)
- At sub seismic slip velocities the displacement after which MSS develop rapidly decreases as normal stress is increased
- MSS are not observed at intermediate velocities ($v = 10^{-4} - 10^{-3} \text{ ms}^{-1}$)
- Our results demonstrate that continuous MSS can be produced at both seismic and sub seismic slip velocities and share similar microstructural characteristics so they cannot be used as reliable indicators of paleoseismic slip



$$W = \tau \cdot v$$

W = Mechanical power density [W/m^2] τ = peak shear stress [MPa] v = slip velocity [ms^{-1}] (Fondriest et al., 2013)

Fondriest, M., Smith, S., Candela, T., Nielsen, S., Mair, K. and Di Toro, G., 2013. Mirror-like faults and power dissipation during earthquakes. *Geology*, 41(11), pp.1175-1178.

Green II, H., Shi, F., Bozhilov, K., Xia, G. and Reches, Z., 2015. Phase transformation and nanometric flow cause extreme weakening during fault slip. *Nature Geoscience*, 8(6), pp.484-489.

Siman-Tov, S., Aharonov, E., Boneh, Y. and Reches, Z., 2015. Fault mirrors along carbonate faults: Formation and destruction during shear experiments. *Earth and Planetary Science Letters*, 430, pp.367-376.

Siman-Tov, S., Aharonov, E., Sagy, A. and Emmanuel, S., 2013. Nanograins form carbonate fault mirrors. *Geology*, 41(6), pp.703-706.

Verberne, B., Plumper, O., Matthijs de Winter, D. and Spiers, C., 2014. Superplastic nanofibrous slip zones control seismogenic fault friction. *Science*, 346(6215), pp.1342-1344.